

# Rheology near jamming - the influence of lubrication forces

Moumita Maiti and Claus Heussinger

*Institute for Theoretical Physics, Georg-August University of Göttingen,  
Friedrich-Hund Platz 1, 37077 Göttingen, Germany*

(Dated: August 17, 2018)

We study, by computer simulations, the role of different dissipation forces on the rheological properties of highly-dense particle-laden flows. In particular, we are interested in the close-packing limit (jamming) and the question if “universal” observables can be identified that do not depend on the details of the dissipation model. To this end, we define a simplified lubrication force and systematically vary the range  $h_c$  of this interaction. For fixed  $h_c$  a cross-over is seen from a Newtonian flow regime at small strain rates to inertia-dominated flow at larger strain rates. The same cross-over is observed as a function of the lubrication range  $h_c$ . At the same time, but only at high densities close to jamming, single-particle velocities as well as local density distributions are unaffected by changes in the lubrication range – they are candidates for “universal” behavior. At densities away from jamming, this invariance is lost: short-range lubrication forces lead to pronounced particle clustering, while longer-ranged lubrication does not. These findings highlight the importance of “geometric” packing constraints for particle motion – independent of the specific dissipation model. With the free volume vanishing at random-close packing, particle motion is more and more constrained by the ever smaller amount of free space. On the other side, macroscopic rheological observables, as well as higher-order correlation functions retain the variability of the underlying dissipation model.

PACS numbers:

## I. INTRODUCTION

The jamming paradigm aims at providing a unified view for the elastic and rheological properties of materials as different as foams, emulsions, suspensions or granular media [1]. Structurally, these systems can all be viewed as dense assemblies of (non-Brownian) particles, and the particle volume fraction plays the role of the coupling constant that tunes the distance to the jamming transition. The usefulness of such a unifying concept hinges on the presence or absence of phenomena that are in some sense “universal”. An important goal then is to delineate these universal aspects of the jamming transition from system-specific properties that depend on microscopic details, the driving mechanism or the preparation protocol.

The elasticity and visco-elasticity of jammed packings of particles have received a lot of attention in the past few years (see e.g. the review [2]). The elastic moduli and their visco-elastic generalizations [3] naturally depend on the specific interaction potential characterising the given particles [4]. However, this variation can be understood in terms of a more fundamental – and universal – relation between inter-particle contacts and volume fraction [5].

The state of things is much less clear when it comes to flowing systems at densities close to the jamming transition. A key complication arises because of the manifold of highly system-specific dissipation mechanisms that characterize the different systems. Dissipation in emulsions and suspensions is primarily of hydrodynamic origin, e.g. in the form of lubrication forces or long-range hydrodynamic interactions. In granular powders, inelastic collisions and dry friction dominate the dissipation [31]. In wet granular media, finally, the breaking of liquid capillary bridges between near-by particles is important [6].

Accordingly, the flowcurves (which constitute the appropriate generalization of the visco-elastic moduli of the packings) display a wide variety of different forms for different systems. At small strainrates (or in the hard-particle limit) Newtonian [7, 27] or Bagnold regimes [8–10] are observed. The associated viscosities diverge at the jamming transition signalling the impossibility of flow due to packing constraints. At larger strainrates jamming is usually associated with shear thinning [11–14] or possibly with shear-banding when attractive forces are present [19]. When inter-particle friction is important hysteretic behavior [15, 16, 18] as well as continuous and discontinuous shear thickening [17, 20–22, 24] have been observed.

At present it is not clear, however, if there can be any hope to explain (at least some of) this broad range of rheological properties on the basis of one or a few generic principles. Progress in this direction has been made, for example, by defining an underlying contact network [7, 25] in analogy to what has been achieved for the jammed packings; or by establishing macro-micro correspondences [26] or scaling relations [27–29] between exponents characterizing different aspects of the jamming singularity.

In this contribution we ask about the influence of different dissipation mechanisms on the flow properties close to jamming. The goal is to identify universal observables that do not depend on the precise nature of the dissipation mechanism, and distinguish them from system-specific observables that do depend on these details. We expand on the results of Ref. [27] where a certain decoupling between the dissipation law and the single particle motion has been observed. To look into this effect in more detail we will define a family of dissipation forces and systematically vary the parameters characterizing this fam-

ily. With this we can implement a crossover from a Newtonian to a Bagnold regime and ask about the sensitivity to these changes on the microscopic level of particle trajectories.

## II. SIMULATION

We study a two-dimensional binary mixture of soft frictionless spheres of mass  $m$ . The system of  $N$  spheres constitute  $\frac{N}{2}$  spheres of diameter  $d$  and  $\frac{N}{2}$  spheres of diameter  $1.4d$ . The particle volume fraction is defined as  $\phi = \frac{\sum_{i=1}^N \pi R_i^2}{L^2}$ , where  $R_i$  is the radius of a particle  $i$ , and  $L$  is the length of the simulation box. The system is sheared along the x-direction with a strain rate  $\dot{\gamma}$  and Lees-Edwards periodic boundary conditions are used.

Particles interact via elastic repulsion and via dissipative forces. Two particles repel each other if they are in overlap with an elastic force,

$$\vec{F}_{\text{el}} = -\vec{n}_{ij}\epsilon_{ij}(1 - \frac{r_{ij}}{r_c}), \quad r_{ij} < d \quad (1)$$

where  $\vec{n}_{ij}$  is the unit vector pointing from particle  $i$  to particle  $j$ , and  $r_{ij}$  is the distance between the two particles. The cut-off  $d = (d_i + d_j)/2$  is set by the diameters of the two interacting spheres. In the small-strainrate limit  $\dot{\gamma} \rightarrow 0$  the average overlap vanishes and the particles effectively behave as hard-spheres ( $\epsilon \rightarrow \infty$ ). In this limit the shear stress is independent of the particle stiffness  $\epsilon$ .

The dissipative force is modeled as

$$\vec{F}_{\text{diss}} = -\zeta \vec{v}_{ij}, \quad r_{ij} < d(1 + h_c), \quad (2)$$

where  $\vec{v}_{ij} = \vec{n}_{ij}[\vec{n}_{ij} \cdot (\vec{v}_i - \vec{v}_j)]$  is the relative normal velocity between interacting particles. The range of the dissipative force  $d(1 + h_c)$  is, in general, taken to be larger than that of the elastic force. We characterize this range by the parameter  $h_c$ , which will be varied systematically in what follows. The model is different from Durian's bubble model for foams [34] mainly due to the presence of these lubrication forces: dissipative forces with a range longer than the elastic forces. Another difference is that the dissipative force in the bubble model is proportional to the total relative velocities

In the limit  $h_c = 0$ , particles see each other only when they overlap. Dissipation is then due to inelastic collisions between particles. This dissipation mechanism corresponds to the case of a dry granular powder [30, 31]. For  $h_c > 0$  particles may interact even without collision, and Eq. (2) can be viewed as a simplified lubrication force, where  $h_c$  plays the role of the range of the lubrication interaction. In the following we will therefore call  $h_c$  the lubrication range.

As discussed our aim here is to understand the role of different dissipation interactions on flow properties. To serve this purpose, we design a model incorporating the features of suspension flow in a simple manner. The model proposed here aims at understanding the possible

underlying mechanisms of flow in the context of critical phenomena at the jamming transition. In real suspensions, hydrodynamic forces have a long-range many-body component. The method of Stokesian dynamics is capable of simulating these effects efficiently for low and intermediate densities [33]. Here, we are interested in high densities, close to the maximal density of random close packing. In this regime, a common assumption is to neglect these long-range hydrodynamic forces and assume them to be efficiently screened by the many surrounding particles. The remaining hydrodynamic effects are then lubrication forces, which only act when particles are separated by a small gap  $h$ . For two interacting ideal hard-spheres, the leading order term ( $h \rightarrow 0$ ) can be written in the form of Eq. (2) with a distance-dependent viscous coefficient  $\zeta(h)$  that diverges upon particle collision,  $\zeta \sim h^{-1}$  [35]. Next to this normal component (squeeze mode) there is also a (subdominant) tangential component of the lubrication force (shear mode). The tangential viscous coefficient diverges logarithmically with the particle gap  $\zeta_t(h) \propto -\log(h)$ . In reality, these divergences are cut-off at small distances set by the surface properties of the particles. In general, neither the microscopic cut-off nor the range of the lubrication force (it is one term in a series) are known. This warrants a detailed investigation into how the functional form of the lubrication interaction affects the flow properties at high densities. To this end we provide Eq. (2) as a simplified model for the lubrication forces.

In most of our simulations we set the viscous coefficient to be constant (up to the range  $h_c$ ) and independent of distance

$$\zeta(h) = \zeta_0, \quad h < dh_c \quad (3)$$

Alternatively, we have used

$$\zeta(h) = \zeta_0 \begin{cases} 1, & r_{ij} < d \\ e^{-h/(dh_c)}, & r_{ij} \geq d \end{cases} \quad (4)$$

with a cut-off at a large value ( $2.5d$ ). It will turn out, however, that these different choices do not affect the rheological properties of the system.

With the forces given above Newton's equations of motion  $m\vec{r} = \vec{F}_{\text{el}} + \vec{F}_{\text{visc}}$  are integrated with a molecular dynamics (md) simulation using LAMMPS [37]. We use md timestep  $\Delta t = 0.01$  and the viscous drag  $\zeta_0 = 2$ . The system size  $N = 1000$  is considered for most of the analysis unless larger system sizes are required. All quantities are expressed in units of  $d$ ,  $\epsilon$ , and  $m$  ( $d = 1$ ,  $m = 1$ ,  $\epsilon = 1$ ).

## III. RESULTS

### A. Close to jamming: $\phi = 0.83$

The rheology of a fluid is primarily described by its flowcurve, i.e. the relation between shear stress  $\sigma$  and

strainrate  $\dot{\gamma}$ . In what follows, we fix the volume-fraction to  $\phi = 0.83$ , which is close to the jamming transition at  $\phi_{rcp} = 0.843$  (random-close packing). The shear stress is calculated using  $\sigma = \sum_i F_{iy}x_i/A$ , where  $F_{iy}$  is  $y$ -component of the total force  $F = F_{el} + F_{diss}$ ,  $A$  is area, and it has dominant contribution from the elastic forces. The particle overlaps that generate these elastic forces are always at least an order of magnitude smaller than the lubrication range. Fig. 1 shows the flowcurves  $\sigma(\dot{\gamma})$  for different lubrication ranges  $h_c \in [0, 0.05]$ .

At the special value  $h_c = 5 \cdot 10^{-4}$  the data is displayed for the two variants of the dissipation model, with  $\zeta$  taken from Eq. (3) or Eq. (4) (open and closed squares). As can readily be seen, the flowcurves are insensitive to this change and therefore independent of the specific functional form for  $\zeta(h_c)$ . As this is also true for the other quantities we will discuss, in the following we only show data with  $\zeta$  taken from Eq.(3).

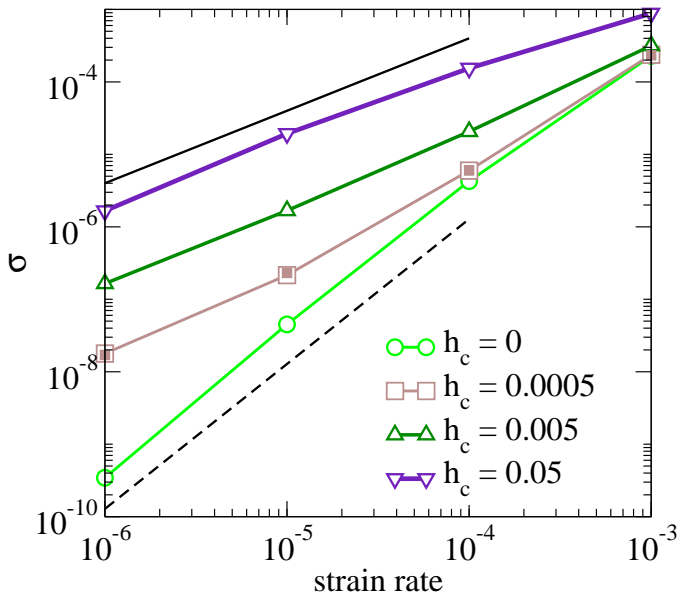


FIG. 1: Flow curves  $\sigma(\dot{\gamma})$  at the volume fraction  $\phi = 0.83$ . Thin (black) lines represent power-laws  $\sigma \propto \dot{\gamma}^\nu$  with exponents  $\nu = 2$  (dashed) and  $\nu = 1$  (solid).

The flowcurves do depend, though, on the *range* of the dissipation force. For  $h_c = 0$  (circles) the shear stress scales quadratically with strainrate,  $\sigma = \hat{\eta}\dot{\gamma}^2$ . In this limit, the dissipative force Eq. (2) only acts when particles overlap, i.e. during a particle collision. This regime is well-known from the flow of granular powders [30, 31]. The quadratic (“Bagnold”) scaling with strainrate can readily be explained by dimensional analysis [36]. Shear stress (in two dimensions) is work done per unit area and the dimensional analysis gives  $\sigma \sim m\dot{\gamma}^2$ , i.e. the effective viscosity is proportional to particle mass,  $\hat{\eta} \sim m$ . Hence, rheology in the limit  $h_c = 0$  is ascribed to inertia (“inertial regime”).

Increasing  $h_c$  from zero, there is a crossover to a second, “viscous regime”, where,  $\sigma = \eta\dot{\gamma}$ , a Newtonian liquid.

uid. Here viscous lubrication forces dominate over inertial forces, and dimensional analysis gives  $\eta \propto \zeta_0$ . The crossover is also seen at a fixed  $h_c$ , from viscous regime at low strainrate to inertial regime at higher strainrate [42]. A similar crossover is also present in experiments [38, 39], and recent simulations [23]. It may also be interpreted in terms of shear-thickening as a consequence of inertial effects, similar to what has been seen in Ref. [21].

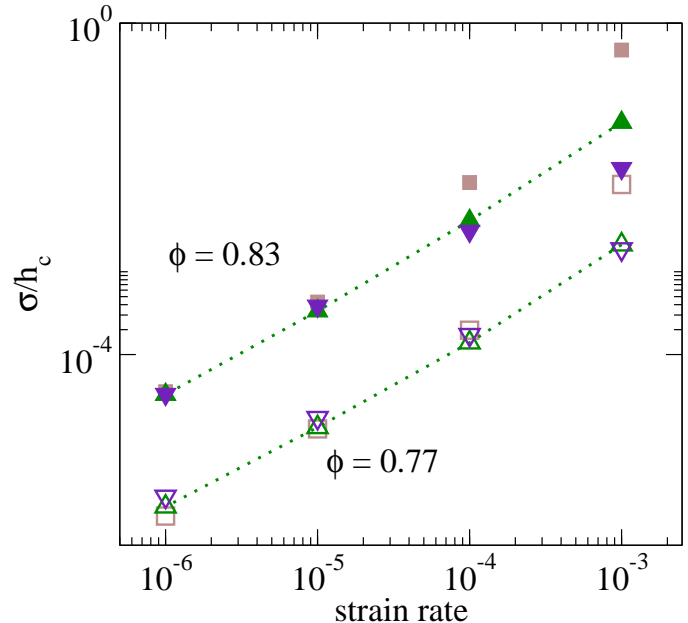


FIG. 2: Flow curves normalized by lubrication range  $h_c$  at densities 0.83 and 0.77. The coloring is the same as in Fig. 1.

Fig. 2 shows that the stress  $\sigma \propto h_c$  in the viscous regime. This scaling can be understood from an energy balance between injected work and dissipated energy. The key ingredient is the  $h_c$ -dependent dissipation volume (area)  $v_d = (\pi d^2)((1+h_c)^2 - 1) \sim \pi d^2 h_c$  ( $h_c$  is dimensionless!). The scaling expression for the energy balance between work and dissipation reads:  $d^2 \sigma \dot{\gamma} \sim \zeta \dot{\gamma}^2 v_d$ , where  $\sigma \dot{\gamma}$  represents the density of work and  $\zeta \dot{\gamma}^2$  the dissipation density. The stress then follows as  $\sigma \sim \zeta \dot{\gamma} h_c$ . Hence, the scaling  $\sigma \propto h_c$ .

Looking in more detail, the energy balance equation can be written as  $\sigma\dot{\gamma} \propto 2\pi\zeta \int dh(d+h) g(h)v^2(h)$ , where  $v^2(h) = \langle v_{ij}^2 \rangle_h$  is the normal component of the relative velocity of two particles  $i$  and  $j$  (as in Eq. (2)) and the average is taken over all interacting particle pairs at a prescribed gap  $h$ . Furthermore,  $g(h)$  is the pair-correlation function.

As can be seen in Fig. 3, the dissipation density  $\zeta g(h)v^2(h)$  is approximately constant and only weakly dependent on  $h$  and  $h_c$ , thus validating the scaling ansatz. Notably, the individual contributions  $g(h)$  and  $v^2(h)$  are not constant and furthermore strongly depend on the lubrication range  $h_c$ . Interestingly, they both obey approximate scaling forms  $v^2(h) = h_c \mathcal{F}(h/h_c) \sim 1/g(h)$  with a scaling function  $\mathcal{F}(x) \approx x^{1/2}$ . Thus, both relative par-

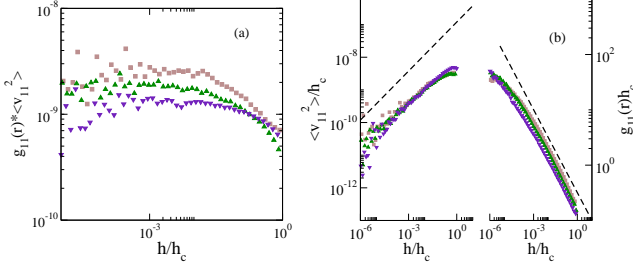


FIG. 3: (a) Average dissipation density vs rescaled gap  $h/h_c \equiv (r - \sigma)/(dh_c)$  for different  $h_c$  (only small-small (11) particle pairs are accounted for). (b) Rescaled relative velocities and pair-correlation function vs. gap  $h/h_c$ . Dashed lines indicate power-law  $x^{1/2}$  and  $x^{-1/2}$ , respectively. The coloring is the same as in Fig. 1. Strain rate is  $\dot{\gamma} = 10^{-5}$ .

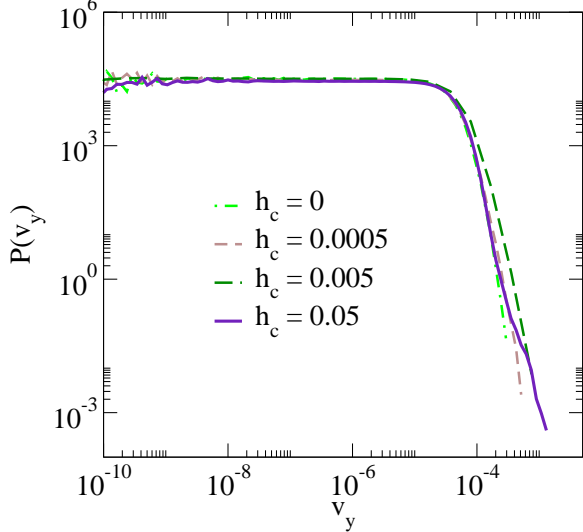


FIG. 4: The distribution function of particle velocities  $|v_y|$  at volume fraction  $\phi = 0.83$ . The strain rate is  $\dot{\gamma} = 10^{-5}$ .

ticle velocities and local structure do vary strongly with dissipation range while dissipation densities does not.

Fig. 4 shows the probability distribution of *single* particle velocities  $v_y$  (gradient component). The velocity component  $v_x$  (flow direction) has both affine and non-affine contributions, while the component  $v_y$  is purely non-affine. So, we look at the distribution of  $v_y$  to avoid mixing of affine and non-affine motion.

Quite surprisingly, and distinct from the relative velocities, the distribution of single-particle velocities hardly changes by changing the range  $h_c$  of the lubrication force [43]. Recall, that at the same time, the flowcurve (Fig. 1) changes by orders of magnitude and even the functional form  $\sigma(\dot{\gamma}) \sim \dot{\gamma}^x$  changes, from  $x = 2$  to  $x = 1$ . Apparently, all these changes can be accomplished with only minimal changes in the statistical properties of the single particle velocities. Below, we will furthermore see that the local particle density behaves similarly (Fig. 8b). Thus, it seems that single-particle (one-point) observ-

ables, and in particular the single-particle velocities are independent of dissipation range  $h_c$ , while higher-order correlations (multi-point observables) are very sensitive to details of the dissipation model.

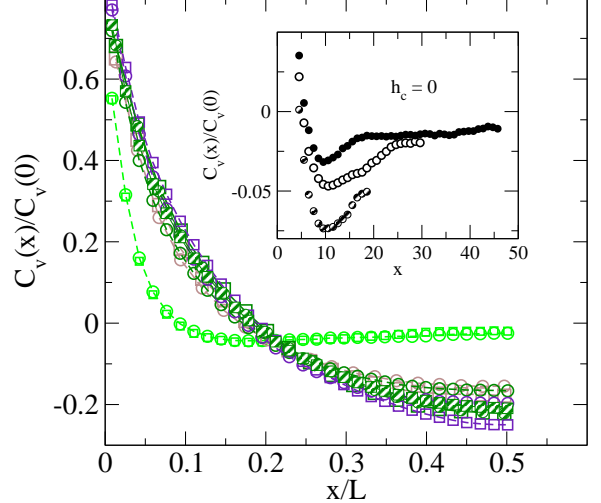


FIG. 5: The velocity spatial correlation  $C_v(x)/C_v(0)$  (see text) at volume fraction  $\phi = 0.83$  for two strainrates  $\dot{\gamma} = 10^{-5}$  (circle) and  $10^{-6}$  (square). Four cases of different  $h_c$  values are shown. Two system sizes  $N = 1000$  (striped) and  $N = 2500$  (open) are shown. The coloring is the same as in Fig. 1. The x-axis is normalized by box-length  $L$ . Inset shows without this normalization for  $h_c = 0$  for three system sizes  $N = 1000$  (striped) 2500 (open), 6000 (filled).

To reinforce this finding we look at a velocity-correlation function. We calculate velocity spatial correlation  $\frac{C_v(x)}{C_v(0)}$ , where  $C_v(dx) = \langle v_y(x; y)v_y(x + dx; y) \rangle$  and  $C_v(0) = \langle v_y^2 \rangle$  the normalization factor. The relative velocities  $v_{ij}$  of interacting particle pairs are related to the short-distance part of this function. We are now interested in the long-distance behavior far beyond the interaction cut-off. Fig. 5 clearly shows that the correlation function changes its behavior qualitatively, when  $h_c$  is increased from zero to finite values. For  $h_c = 0$  it has a minimum at a certain distance that is independent of system-size (see inset). With lubrication interactions the minimum quickly disappears and the correlation function rather monotonically decays with a length-scale that depends on the system-size. Quite similar results on the correlation function have been reported in a related system [3]. There, two different dissipation forces have been compared in the context of Durian's bubble model [34].

These findings throw an interesting light on the role of dissipative and elastic forces in this system. Recall, that the stress is independent of particle stiffness  $\epsilon$ , i.e. particles effectively behave as hard spheres ( $\epsilon \rightarrow \infty$ ): the elastic forces then very effectively serve to reinforce the volume exclusion between nearby particles. The free volume of a hard-sphere system vanishes at random-close packing, thus, particle motion is more and more constrained by the ever smaller amount of free space, as random close

packing is approached from below. It is this geometric ‘‘singularity’’ that provides strong constraints for particle motion. In previous work [32], we have shown how single-particle velocities  $\langle v_y^2 \rangle$ , as a result of these constraints, actually *diverge*, when RCP is approached. Such a geometric mechanism is independent of the specific dissipative force, and therefore of the dissipation range  $h_c$ , as observed in Fig.4. The remaining role of dissipation then is to determine the higher-order contributions to the particle motion, and indeed, the *amount of dissipated energy* along geometrically predetermined trajectories.

Naturally, this picture only works, if the steric effects of volume exclusion provide strong constraints on particle motion. Thus, the closer to random-close packing the better. This was shown explicitly in Ref. [27], where the critical density was approached up to  $\phi_{\text{rcp}} - \phi = 0.003$ . In the following section we will see how by *reducing* the density and going away from close packing, the newly available space can be used.

### B. Away from jamming: $\phi = 0.77$

We fix the packing-fraction  $\phi = 0.77$  away from random close packing. Fig. 6(a),(b) show the flowcurves and the associated single-particle velocity distributions. Like at  $\phi = 0.83$ , the same crossover between inertial and viscous regime is observed. Also the scaling with  $h_c$  in Fig. 2 is present with small deviations. Unlike at  $\phi = 0.83$ , however, the velocity probability distribution function is changing with  $h_c$  (Fig. 6(b)).

This highlights that the single-particle motion is no longer governed only by the geometry of packings. Particles now have enough space to move. The geometric constraints are relaxed and particle motion is a result of a complex interplay of elastic and dissipative forces.

Looking more closer into the variation of the velocity distribution function in Fig. 6(b), one observes that the distribution function is non-monotonic with the lubrication range  $h_c$ . The tail is enhanced at small  $h_c$ , indicating faster movement of particles. Interestingly by further increasing  $h_c$  this enhancement goes away and particle velocities are almost the same as at  $h_c = 0$ . This trend is clearly visible in the second moment of the distribution ( $\langle v_y^2 \rangle$ ), which we show in the inset of Fig. 6(b). Indeed, typical non-affine velocities are maximal at intermediate values of the lubrication range.

There may be a change in structure coupled to this velocity maximum so we look at snapshots. Fig. 7 shows two snapshots one at  $h_c = 0$ , the other at  $h = 5 \cdot 10^{-4}$ . The structure at  $h_c = 0$  is homogeneous whereas at  $h_c = 5 \cdot 10^{-4}$  it displays density fluctuations and particle clustering.

We have quantified these density fluctuations by calculating local Voronoi area using a ‘‘generalized Voronoi’’ algorithm [40]. The density is large if the area is small and *vice versa*. Fig. 8(a) shows the probability distributions of local Voronoi area of the smaller particle for

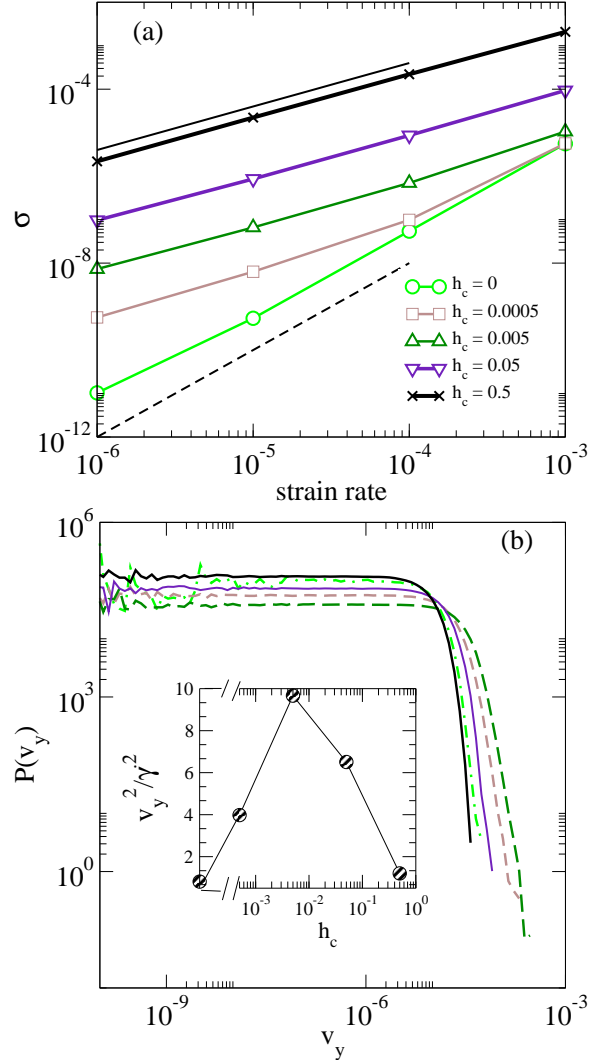


FIG. 6: (a) Flowcurves for volume fraction  $\phi = 0.77$ . (b) The distribution function of  $|v_y|$  at volume fraction  $\phi = 0.77$ . Coloring is the same as Fig.1 (in addition, data for  $h_c = 0.5$  (black line and cross symbol) is shown). Strain rate is  $\dot{\gamma} = 10^{-5}$ . Inset in panel (b) shows the second moment  $\langle v_y^2 \rangle$  vs. lubrication range  $h_c$ , where  $y$ -axis is divided by  $\dot{\gamma}^2$ .

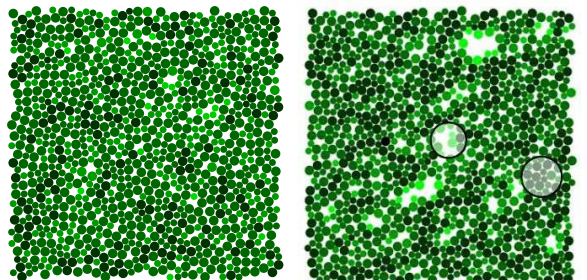


FIG. 7: Snapshots for (a)  $h_c = 0$  and (b)  $h_c = 0.005$ . Volume fraction  $\phi = 0.77$ . Coloring is done from high(dark) to low(light) local density. Possible clusters or ‘holes’ are highlighted by circles.

different lubrication ranges  $h_c$ . We show data of one component as the distribution is qualitatively similar for both particle sizes, except the peak position is different. A broad tail is observed for small  $h_c$  which is a clear indication of large voids and associated particle clustering. The tail comes back to normal ( $h_c = 0$ ) behavior by further increasing  $h_c$ . This implies that clustering disappears by increasing  $h_c$ . The distribution of local density is therefore non-monotonic, and behaves much in the same way as the velocity distribution function Fig. 6(b).

Lubrication-induced clustering should be taken as a consequence of the minimization of energy dissipation. Indeed, forming clusters is expected to reduce the relative motion of nearby particles, thus reducing their dissipation. However, we have also seen that particle clustering comes at the cost of enhanced single-particle motion (Fig. 6(b)). This may seem paradoxical, at first. However, previous work on related systems have shown how clusters can be viewed as particles with renormalized diameter  $\tilde{d}$  [17, 27]. The velocity scale of such a particle is  $v \sim \dot{\gamma}\tilde{d}$  (on dimensional grounds), and thus increases quite naturally with the size of the particle/cluster. With the data taken from the inset of Fig. 6(b) we can estimate the cluster size('hole' size) to be on the order of  $\tilde{d} \sim 3$ . While this seems to be in rough agreement with the size of the inhomogeneities seen in Fig. 7, care must be taken and cluster size should be measured directly to quantitatively confirm this speculation.

Finally, note that at  $\phi = 0.83$  the distribution of Voronoi areas is nearly independent of the lubrication range  $h_c$  (Fig. 8(b)). A small enhancement of the tail can be seen indicating a very weak clustering also at the higher density. This may explain the weak dependence of the velocity distribution function on  $h_c$  as seen in Fig. 4. This effect is expected to vanish upon increasing the density further towards random-close packing.

To conclude, at densities away from the close-packing threshold the motion of particles is governed not only by steric constraints but by a complex interplay of conservative and dissipative forces. In particular, we observe that short-range lubrication forces induce particle clustering. Longer-range lubrication does not lead to clustering. Rather several observables, like the local density or the velocity distribution, have much the same form as without any lubrication forces (i.e. with only inelastic collisions as dissipation mechanism).

#### IV. DISCUSSION AND CONCLUSION

The goal of this work was to investigate the role of dissipative forces for the rheological properties of highly dense particulate flows. The question is if and under what circumstances “universal” observables can be identified that do not depend on the details of the dissipative model. To answer this question, we defined a simplified lubrication force between near-by particles, and systematically varied the range  $h_c$  of this interaction.

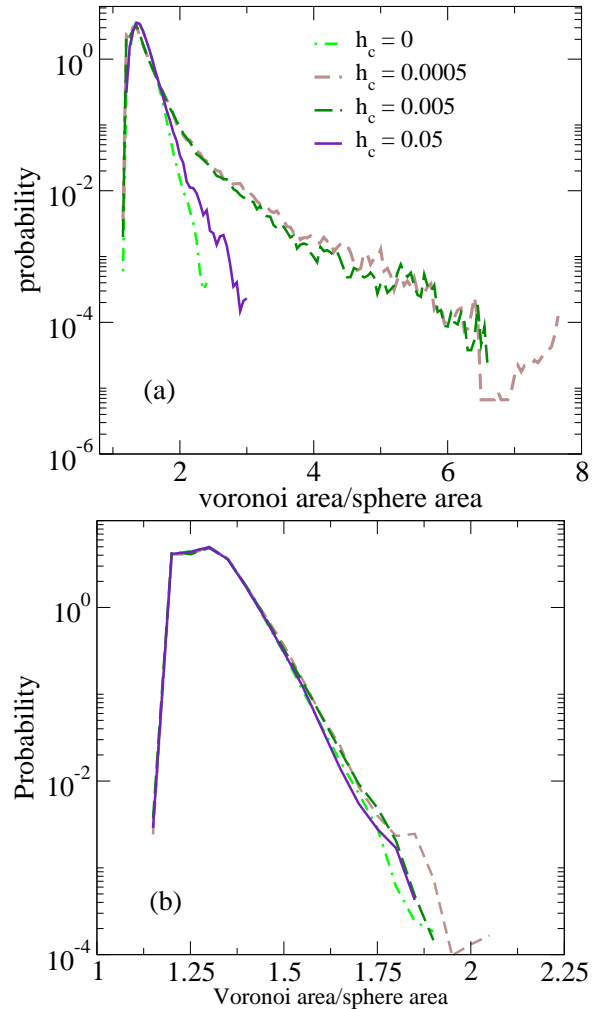


FIG. 8: The probability distribution of local Voronoi area (inverse local density) at  $\dot{\gamma} = 10^{-5}$ . (a)  $\phi = 0.77$ , (b)  $\phi = 0.83$ . The Voronoi area is normalized by respective sphere area.

On the level of the flowcurves we observe a transition from a Bagnold to a Newtonian regime by changing either  $\dot{\gamma}$  or  $h_c$ . The stress can be written as

$$\sigma = \eta_N h_c \dot{\gamma} + \eta_B \dot{\gamma}^2 \quad (5)$$

with volume-fraction dependent “viscosities”  $\eta_N$  and  $\eta_B$ . While from our simulations we cannot make any definite statement about the volume-fraction dependence, from previous work one expects a power-law divergence at the close-packing threshold, thus  $\eta_N \sim (\phi_{\text{rcp}} - \phi)^{-\beta}$  and  $\eta_B \sim (\phi_{\text{rcp}} - \phi)^{-\alpha}$  with  $\alpha \approx 4$  and  $\beta \approx 2$  [12, 27]. This entails a crossover strainrate  $\dot{\gamma}_c \sim \delta\phi^{\alpha-\beta} h_c$  that is vanishing at  $\phi_c$ . The crossover stress  $\sigma_c \sim \delta\phi^{\alpha-2\beta}$  is expected to be only weakly density dependent. Note, that qualitatively similar results have been found in the experiments of Ref. [39], albeit over an extended volume-fraction range, where the simple power-law dependence is not expected to hold anymore.

Going beyond the characterization of the flowcurves

we found that systems at random-close packing are only weakly sensitive to the lubrication range. In particular, the single-particle velocity and the local density distributions are nearly unchanged by varying  $h_c$  and therefore serve as candidates for “universal” behavior. We attribute this invariance to the strong geometrical constraints of excluded volume which do not allow particles to react to changes in the dissipative force.

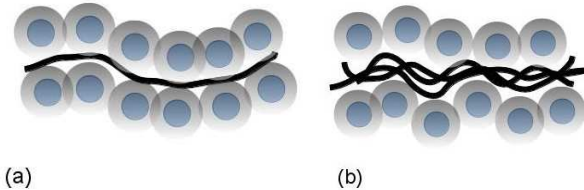


FIG. 9: Schematic of possible paths arising from geometric aspects. A mobile test particle passing through an immobile environment. A high densities the narrow channel in (a) very effectively restricts the motion of the mobile particle. At lower densities (b) many different passages through the channel are possible. The bigger sized (opaque) circles represent the excluded volume for the motion of the mobile test particle.

The simple schematic in Fig. 9 illustrates the underlying idea. The geometric constraints of a dense immobile environment force a single mobile particle to move along a well defined trajectory through a narrow channel. Dissipative forces only determine the fine-details of the transit encoded, for example, in the relative particle motion during collisions. More generally, it seems that changes in the dissipation show up only in higher-order correlation functions as observed in spatial velocity correlation, but not in the single particle motion. Dissipation, then, decides upon the amount of energy that is necessary to push the particle through the channel.

At densities away from close-packing, geometrical con-

straints are weak and particles *do* respond to the dissipation mechanism (like in the wide channel of Fig.9(b) ). The qualitative features of this response strongly depend on lubrication range  $h_c$ . For small  $h_c$  we find pronounced particle clustering evident, for example, in the distribution of local Voronoi volumes.

Particle clustering as a result of lubrication forces is well known in the literature of dense suspension flows [41] and are believed to be responsible for the phenomenon of shear-thickening. Clusters form because particles that are pushed together by the flow experience the high viscous coefficient of the lubrication force. Shear thickening then occurs, because smaller and smaller inter-particle gaps are probed when the strainrate is increased. The lubrication force keeps particles together, the repulsive force drives particles apart. This delicate balance is shifted towards closer gaps, when strainrate is increased. In our simplified model, no such balance at finite gaps is possible. As a consequence, particles either “fully” cluster or they don’t cluster at all. There is no effect of strainrate. Rather, we view clustering as a possibility for the particles to better utilize the free space in order to *reduce* energy dissipation and thus viscosity (as compared to the unclustered state).

Finally, we have shown that long-range lubrication forces do not lead to clustering. Apparently, long-range lubrication forces are very effectively screened and only act as a kind of mean field. It would be tempting to speculate that the full long-range hydrodynamic interactions share the same fate at high enough particle densities as our simplified lubrication interactions do.

## Acknowledgments

We acknowledge financial support by the DFG via the Emmy Noether program (He 6322/1-1).

---

[1] A. J. Liu and S. R. Nagel, *Nature* **396**, 21 (1998).

[2] M. van Hecke, *J. Phys.: Cond. Matt.* **22**, 033101 (2010).

[3] B. P. Tighe, *Phys. Rev. Lett.* **109**, 168303 (2012), URL <http://link.aps.org/doi/10.1103/PhysRevLett.109.168303>.

[4] C. S. O’Hern, L. E. Silbert, A. J. Liu, and S. R. Nagel, *Phys. Rev. E* **68**, 011306 (2003).

[5] A. J. Liu, S. R. Nagel, W. van Saarloos, and M. Wyart, *The jamming scenario – an introduction and outlook* (Oxford University Press, 2010), chap. 9.

[6] S. Strauch and S. Herminghaus, *Soft Matter* **8**, 8271 (2012), URL <http://dx.doi.org/10.1039/C2SM25883H>.

[7] E. Lerner, G. Düring, and M. Wyart, *Proc. Natl. Acad. Sci. USA* **109**, 4798 (2012), <http://www.pnas.org/content/109/13/4798.full.pdf+html>, URL <http://www.pnas.org/content/109/13/4798.abstract>.

[8] F. da Cruz, S. Emam, M. Prochnow, J.-N. Roux, and F. Chevoir, *Phys. Rev. E* **72**, 021309 (2005).

[9] M. Trulsson, B. Andreotti, and P. Claudin, *Phys. Rev. Lett.* **109**, 118305 (2012), URL <http://link.aps.org/doi/10.1103/PhysRevLett.109.118305>.

[10] F. Boyer, E. Guazzelli, and O. Pouliquen, *Phys. Rev. Lett.* **107**, 188301 (2011), URL <http://link.aps.org/doi/10.1103/PhysRevLett.107.188301>.

[11] P. Olsson and S. Teitel, *Phys. Rev. Lett.* **99**, 178001 (2007).

[12] M. Otsuki and H. Hayakawa, *Physical Review E (Statistical, Nonlinear, and Soft Matter Physics)* **80**, 011308 (pages 12) (2009).

[13] K. N. Nordstrom, E. Verneuil, P. E. Arratia, A. Basu, Z. Zhang, A. G. Yodh, J. P. Gollub, and D. J. Durian, *Phys. Rev. Lett.* **105**, 175701 (2010), URL <http://link.aps.org/doi/10.1103/PhysRevLett.105.175701>.

[14] J. Paredes, M. A. J. Michels, and D. Bonn, *Phys. Rev. Lett.* **111**, 015701 (2013), URL <http://link.aps.org/doi/10.1103/PhysRevLett.111.015701>.

[15] M. Otsuki and H. Hayakawa, *Phys.*

Rev. E **83**, 051301 (2011), URL <http://link.aps.org/doi/10.1103/PhysRevE.83.051301>.

[16] M. P. Ciamarra, R. Pastore, M. Nicodemi, and A. Coniglio, Phys. Rev. E **84**, 041308 (2011), URL <http://link.aps.org/doi/10.1103/PhysRevE.84.041308>.

[17] C. Heussinger, Phys. Rev. E **88**, 050201(R) (2013).

[18] M. Grob, C. Heussinger, and A. Zippelius, arXiv:1311.5416 (2013).

[19] E. Irani, P. Chaudhuri, and C. Heussinger, arXiv:1312.4819 (2013).

[20] R. Seto, R. Mari, J. F. Morris, and M. M. Denn, PRL in press, arXiv:1306.5985.

[21] N. Fernandez, R. Mani, D. Rinaldi, D. Kadau, M. Mosquet, H. Lombois-Burger, J. Cayer-Barrioz, H. J. Herrmann, N. D. Spencer, and L. Isa, Phys. Rev. Lett. **111**, 108301 (2013), URL <http://link.aps.org/doi/10.1103/PhysRevLett.111.108301>.

[22] A. Fall, N. Huang, F. Bertrand, G. Ovarlez, and D. Bonn, Phys. Rev. Lett. **100**, 018301 (2008), URL <http://link.aps.org/doi/10.1103/PhysRevLett.100.018301>.

[23] D. Vägberg, P. Olsson, and S. Tietel, arXiv:1311.4902v1 (2013).

[24] E. Brown and H. M. Jaeger, Phys. Rev. Lett. **103**, 086001 (2009), URL <http://link.aps.org/doi/10.1103/PhysRevLett.103.086001>.

[25] C. Heussinger and J.-L. Barrat, Phys. Rev. Lett. **102**, 218303 (2009).

[26] P. Jop, V. Mansard, P. Chaudhuri, L. Bocquet, and A. Colin, Phys. Rev. Lett. **108**, 148301 (2012), URL <http://link.aps.org/doi/10.1103/PhysRevLett.108.148301>.

[27] B. Andreotti, J.-L. Barrat, and C. Heussinger, Phys. Rev. Lett. **109**, 105901 (2012), URL <http://link.aps.org/doi/10.1103/PhysRevLett.109.105901>.

[28] B. P. Tighe, E. Woldhuis, J. J. C. Remmers, W. van Saarloos, and M. van Hecke, Phys. Rev. Lett. **105**, 088303 (2010).

[29] P. Olsson and S. Teitel, Phys. Rev. Lett. **109**, 108001 (2012), URL <http://link.aps.org/doi/10.1103/PhysRevLett.109.108001>.

[30] C. S. Campbell, *Ann. Rev. Fluid. Mech.* **22**, 57 (1990).

[31] H. J. Hermann, J.-P. Hovi and S. Luding *Physics of Dry Granular media* (Kluwer Academic Publishers, Dordrecht, 1998).

[32] Heussinger, C., Berthier, L., and Barrat, J.-L., EPL **90**, 20005 (2010), URL <http://dx.doi.org/10.1209/0295-5075/90/20005>.

[33] J. F. Brady and G. Bossis, *Ann. Rev. Fluid. Mech.* **20**, 111 (1988).

[34] D. J. Durian, *Phys. Rev. E* **55**, 1739 (1997).

[35] R. C. Ball and J. R. Melrose, *Physica A* **247**, 444 (1997).

[36] G. Lois, A. Lemaitre and J. M. Carlson, *Phys. Rev. E* **72**, 051303 (2005).

[37] <http://lammps.sandia.gov/index.html>

[38] N. Huang, G. Ovarlez, F. Bertrand, S. Rodts, P. Coussot, and D. Bonn *Phys. Rev. Lett.* **94**, 028301 (2005).

[39] A. Fall, A. Lemaitre, F. Bertrand, D. Bonn, and G. Ovarlez *Phys. Rev. Lett.* **105**, 268303 (2010).

[40] M. Maiti, A. Lakshminarayanan, and S. Sastry *Eur. Phys. J. E* **36**:5 (2013).

[41] N. J. Wagner and J. F. Brady, *Phys. Today* **62**, 27 (2009).

[42] The slight leveling off in the flowcurves at large strain-rates  $\dot{\gamma} \approx 10^{-3}$  is due to the finite stiffness of the particles  $\epsilon < \infty$ . This will not be discussed here.

[43] Small variations are visible in log-lin representation, especially what regards the height of the plateau [27].